Sensors and Actuators B 243 (2017) 311–325

Contents lists available at ScienceDirect

Sensors and Actuators B: Chemical

journal homepage: www.elsevier.com/locate/snb

Photonic crystal fiber based plasmonic sensors

Ahmmed A. Rifat[a], Rajib Ahmed[b], Ali K. Yetisen[c,d], Haider Butt[b], Aydin Sabouri[b], G. Amouzad Mahdiraji[e], Seok Hyun Yun[c,d], F.R. Mahamd Adikan[a,*]

[a] Integrated Lightwave Research Group, Department of Electrical Engineering, Faculty of Engineering, University of Malaya, Kuala Lumpur-50603, Malaysia
[b] Nanotechnology Laboratory, School of Engineering, University of Birmingham, Birmingham B15 2TT, UK
[c] Harvard Medical School and Wellman Center for Photomedicine, Massachusetts General Hospital, 65 Landsdowne Street, Cambridge, MA 02139, USA
[d] Harvard-MIT Division of Health Sciences and Technology, Massachusetts Institute of Technology, Cambridge, MA 02139, USA
[e] Faculty of Engineering, Taylor's University, Selangor, Subang Jaya-47500, Malaysia

ARTICLE INFO

Article history:
Received 26 July 2016
Received in revised form
20 November 2016
Accepted 22 November 2016
Available online 30 November 2016

Keywords:
Surface plasmon resonance
Photonic crystal fibers
Optical fiber sensors
Biosensors

ABSTRACT

The development of highly-sensitive miniaturized sensors that allow real-time quantification of analytes is highly desirable in medical diagnostics, veterinary testing, food safety, and environmental monitoring. Photonic Crystal Fiber Surface Plasmon Resonance (PCF SPR) has emerged as a highly-sensitive portable sensing technology for testing chemical and biological analytes. PCF SPR sensing combines the advantages of PCF technology and plasmonics to accurately control the evanescent field and light propagation properties in single or multimode configurations. This review discusses fundamentals and fabrication of fiber optic technologies incorporating plasmonic coatings to rationally design, optimize and construct PCF SPR sensors as compared to conventional SPR sensing. PCF SPR sensors with selective metal coatings of fibers, silver nanowires, slotted patterns, and D-shaped structures for internal and external microfluidic flows are reviewed. This review also includes potential applications of PCF SPR sensors, identifies perceived limitations, challenges to scaling up, and provides future directions for their commercial realization.

Contents

* Corresponding author.
E-mail address: rafiq@um.edu.my (F.R.M. Adikan).

http://dx.doi.org/10.1016/j.snb.2016.11.113
0925-4005/

1. Introduction

Surface plasmon resonance (SPR) sensors have attracted lots of interests due to their unique capabilities such as high sensitivity and wide range of applications in environment monitoring [1], food safety [2,3], water testing [4], liquid detection [5,6], gas detection [7,8], biosensing [9,10], and medical diagnostics [11], including drug detection [12,13], bioimaging [14], biological analyte [15,16], and chemical detection [16–19] (Fig. 1). SPR effects are also utilized in optoelectronic devices such as optical tunable filters [20,21], modulators [22,23], SPR imaging [24,25], and thin-film thickness monitoring [26,27]. Besides the SPR techniques some other optical sensing techniques are also available such as microring resonators, waveguides, and resonant mirror [28,29]. In 1950s, surface plasmons (SPs) were theoretically introduced by Ritchie [30]. Based on SPs using the attenuated total reflection (ATR) method, prism coupled SPR Otto configuration was studied by Otto [31], where the prism and plasmonic metal layer were separated by a dielectric (sample) medium. The sensing technique in this study was quite sophisticated as it was required to maintain a finite gap between the prism and metallic layer. The Otto configuration was upgraded by Kretschmann setup, where the prism and metallic layer were in direct contact [32]. To date, Kretschmann and Otto configurations have been among top popular techniques for generating the surface plasmon waves (SPWs). By matching the frequency of incident photons and surface electrons, free electrons are resonating which results in generation and propagation of SPW along the metal-dielectric interface. [33,34]. The fundamental principle of conventional SPR sensors are also described (Supporting Information, Fig. S1). In the 1980s, a SPR sensor was experimentally demonstrated for chemical and biological detection [15]. SPR sensors require a metallic layer that enables transport of large amount of the free electrons. These free electrons are contributing in negative permittivity, which is essential for plasmonic materials. Conventional prism based Kretschmann setup is widely used for SPR sensors, where a prism coated with plasmonic materials is used [18]. As dielectric refractive index (RI) is altered, the propagation constant of the surface plasmon mode is altered which results in changing the coupling conditions or properties of light wave and SPW [16].

Although the performance of prism based SPR sensors (Kretschmann setup) is robust, they are suffering from bulky configuration due to the required optical and mechanical components. These requirements limit the optimization and practical application of these devices at point-of-care settings [18]. The bulky optomechanical components required for the angular interrogation in these devices are also at high costs. Commercial SPR systems such as Biacore, GE Healthcare are also not competitive compared to other devices for industrial application. The conventional SPR sensors are not suitable for field-based applications as a results of moving optical and mechanical parts [18]. The limitations of conventional SPR sensors led to emerging the conventional optical fiber based SPR sensor for chemical sensing applications in the 1990s [17]. There have been various configurations proposed for optical fiber based SPR sensors to provide wider operating range and higher resolution [35–38]. However, optical fiber based SPR sensors are required to direct the incident light at a narrow angle. A planar photonic crystal waveguide-based SPR biosensor was reported where the low refractive index analyte was used for matching the phases [39]. In late 20s, the microstructured optical fiber (MOF) based SPR was proposed [40]. To date, numerous PCF SPR sensors have been demonstrated with different configuration of PCF structures which altering the prism [41–60]. PCF based SPR sensing are capable to be miniaturized. Harnessing its advantages such as small size, ease in light launching, single-mode propagation and ability in controlling evanescent field penetration have made PCF as a promising candidate for SPR sensing [46,47]. However, the reported PCF based SPR sensor structures are not practical from fabrication point of view. As a result, reported PCF SPR sensors were mainly investigated either numerically or analytically. Finite Element Method (FEM) is widely used to numerically investigate the sensing performance. Moreover, analytical approaches such as wavelength and amplitude interrogation method are often used to analyze the sensing performance of these sensors.

The purpose of this review is to (i) discuss conventional prism and fiber based SPR sensing, and describe their drawbacks, (ii) demonstrate how SPR technology fits into the existing PCF sensing, (iii) illustrate various proposed structures and development in layers engineering for improving the sensing performance and also reducing fabrication complexity, and (iv) highlight the current gaps in this field and provide potential solutions. The scope of this review consists of state-of-the-art techniques for the PCF SPR sensors, and their potential applications in public health and industrial setting. It also discusses optical properties of plasmonic materials (gold, silver, copper, graphene and aluminum), metal coating techniques, and their limitations in high sensing performance achievement. Moreover, the sensing performance (RI range, amplitude and wavelength interrogation sensitivity, resolution) of the reported technologies are reviewed.

2. Optical fiber based surface plasmon resonance sensors

2.1. Conventional optical fiber based SPR sensors

Conventional optical fibers are widely used instead of prism in SPR sensors. Transmission and reflection based fiber optic probes have been reported for various sensing applications [55]. Fiber optics based sensors utilize the total internal reflection (TIR) to guide the light for sensing through SPR method. For the transmission based probe, cladding consists of a metal layer and immobilized ligands to detect the unknown concentration of an analyte. In the reflection based method, the end of fiber probe has a mirror to reflect the signal back to the fiber. Transmission method is widely used for fiber based SPR sensors, where the plasmonic metal layer or nanoparticles is placed in an etched cladding region [35–38,61–64]. Various types of fiber optic based SPR sensors including tapered fibers [65,66], D-type fibers [67], Single mode Fibers (SMFs) [68], Multi-mode Fibers (MMFs) [69], Bragg-grating fibers [70], Wagol wheel fibers [71], and H-shaped fibers [72] have been studied. However, the performance of the sensors can be enhanced by modifying the structural parameters/properties of an optical fiber [55]. Recently, Liu et al., utilize the fiber optic based SPR sensors combined with smartphone technologies for imaging and health monitoring applications (Fig. 2a(i)) [73] by using sodium chloride solution with varying RIs ranging from 1.328–1.351 (Fig. 2a(ii)). Abbe refractometer was used to calibrate the sodium chloride solution along with a mini pump to characterize the sensitivity and solution compounds. A low-cost portable smartphone-based fiber optic glycerol SPR sensor was demonstrated by Bremer (Fig. 2b) [74]. Glycerol solution was used to examine the sensor performance resulting in a sensitivity of 5.96×10^{-4} refractive index unit (RIU)/pixel in the range of 1.33–1.36. Fiber optic based label-free biosensors at low-costs were reported for DNA–protein interactions and DNA hybridization measurement by Pollet (Fig. 2c) [75].

Fiber optic based localized SPRs (LSPR) were demonstrated for the purpose of analyzing the antibody-antigen reaction of interferon-gamma (Fig. 2d) [76]. Fiber end was concentrated with the gold NPs and the sensor sensitivity was increased by controlling the density of nanoparticles. The performance comparisons of

Fig. 1. Applications of surface plasmon resonance sensors.

Table 1
Performance comparisons of conventional optical fiber and PCF based SPR sensors.

Characteristics	Wavelength (nm)	RI Range	Sensitivity (nm/RIU)	Resolution (RIU)	Ref.
Fiber optic SPR sensor for the IR region using ITO	1000–1200	1.2–1.21	1310	–	[62]
Tapered fiber optic based SPR sensor in visible range	450–670	1.3328–1.3623	2000	–	[65]
Wagon wheel fiber based SPR sensor	550–730	1.33–1.36	1535	6.5×10^{-6}	[71]
Fiber optic based SPR sensor coated with ITO-Au biolayers	500–650	1.30–1.35	1929	–	[77]
Metal/graphene/MoS_2 coated fiber optic based SPR sensor	550–800	1.330–1.332	6200	–	[78]
Fiber optic based SPR sensor using ZnO thin film	450–700	1.30–1.37	3161	–	[79]
Tapered fiber optic based SPR sensor	450–800	1.333–1.342	8545	–	[80]
Indium Nitride (InN) coated fiber optic based SPR sensor	400–1600	1.30–1.40	4493	–	[81]
Experimentally demonstrated Graphene based fiber optic based SPR biosensor	500–670	1.3326–1.3497	414	–	[82]
Gold wire based PCF SPR sensor	1600–2000	1.30–1.79	3233	3.09×10^{-5}	[83]
D-shaped PCF based SPR sensor	1005–1550	1.43–1.46	9000	1.30×10^{-5}	[84]
External PCF SPR sensing approach	550–820	1.33–1.37	4000	–	[85]
Highly birefringence microstructured fiber based SPR sensor	540–660	1.33–1.34	3100	–	[86]

the conventional fiber optic and PCF based SPR sensors are shown in Table 1.

2.2. Advantages of PCF over prism and conventional optical fibers

PCFs consist of a core and cladding similar to a conventional optical fiber, but the cladding region in PCFs have a periodic air-holes which managing the light propagation [87,88]. Light propagating through the PCFs follows the modified TIR or photonic band gap (PBG) effects [89,90]. By modifying air holes geometries and altering the number of rings light propagation can be controlled. Unique capabilities of PCFs have opened a window to overcome the conventional prism and optical fiber based SPR sensors problems. PCF SPR sensors are also compact and can be incorporated in microscales. Having the advantage of flexibility in design, PCFs geometry can be optimized for achieving the optimum evanescent field. For instance, the core-guided leaky-mode propagation can be controlled by using different types of PCF structures such as hexagonal, square, octagonal, decagonal, hybrid, and their guiding properties can be improved by changing its geometry [72,91]. By optimizing the core-cladding diameter and position, the propagation of light in single mode can be obtained. Single mode PCFs show narrow-band resonance peak results in enhancing the sensitivity [92]. Sensing range and sensitivity can be enhanced by optimizing the structural parameters of the device.

2.3. Sensing mechanism of PCF SPR sensor

PCF based SPR sensors working principle is based on evanescent field. By propagating beam of photons through the core, electromagnetic field would partially penetrate into the cladding region. In PCF SPR sensors, evanescent field penetrates into the cladding region and interacts with the plasmonic metal surface, which excites the free electrons of the surface. When the evanes-

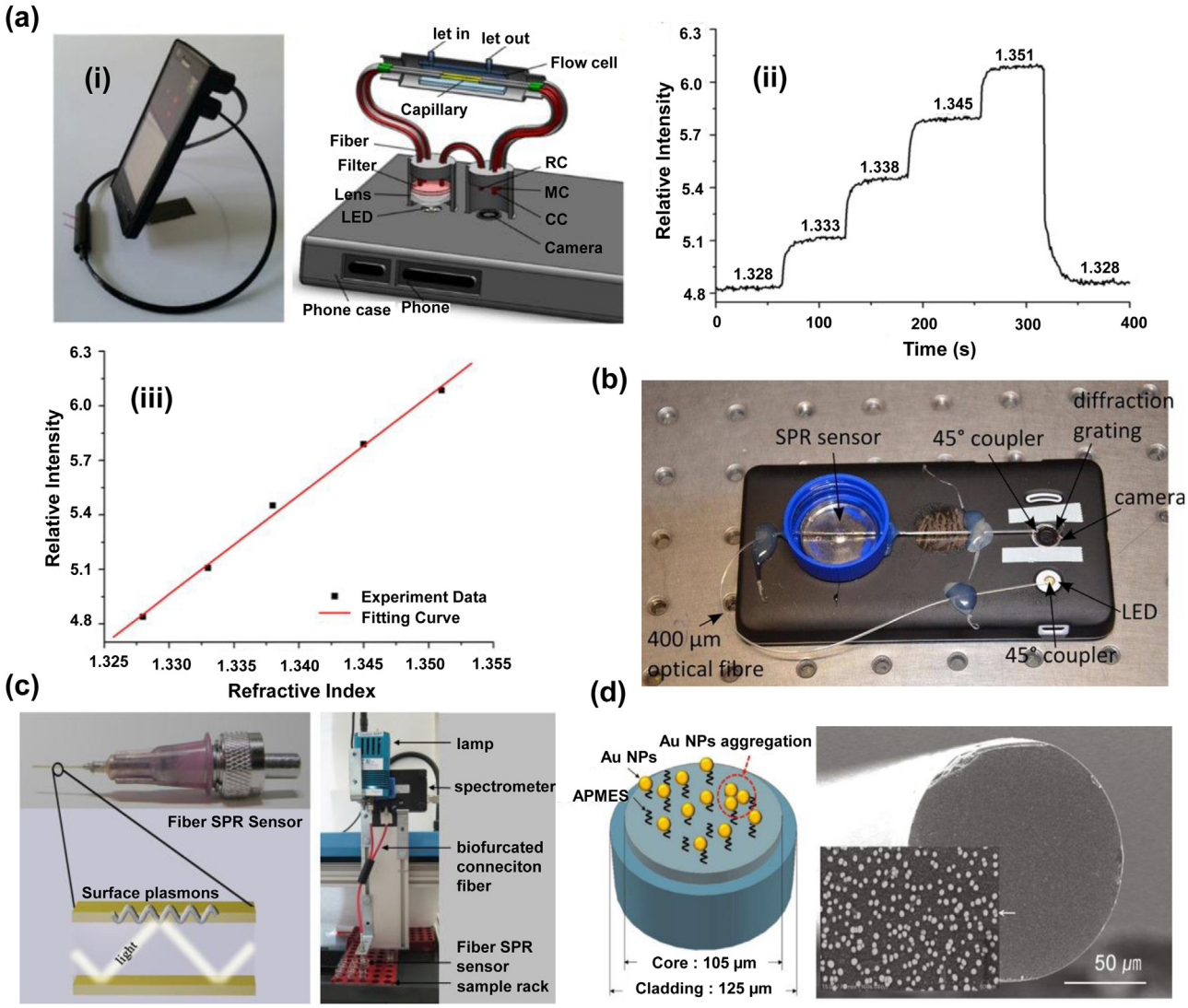

Fig. 2. Fiber optic based SPR sensors. (a) (i) Smartphone-based imaging sensor, (ii) time response with varying RI 1.328-1.351 and (iii) linear fitting of Relative intensity vs refractive index. (b) Smart-phone based SPR sensor for pregnancy test. (c) DNA hybridization and DNA–protein interaction measurement, and (d) LSPR for measuring the concentration of nanoparticles.

cent field and the free electrons of the surface frequencies are matched, the electrons start resonating which results in surface plasmon wave generation. The generated wave is propagated along the metal-dielectric surface interface. This phenomena is known as the resonance condition results in creating a narrow-band loss peak, which is sensitive to the adjacent dielectric medium of metal layer. Resonance occurs when the real effective refractive index (n_{eff}) of core-guided mode and surface plasmon polaritons (SPP) mode values are overlapped. At resonance condition, maximum energy transfers from the core-guided mode to the SPP mode. Due to the change of refractive index of dielectric medium (sample), n_{eff} of SPP changes results in the reducing resonance peak and shift in resonance wavelength. This indicates that the phase matching wavelength is altered depending on the refractive index of sample/analyte. Unknown concentration of a sample can be detected by observing the variation of loss in peak due to the change of analyte's refractive index. Wavelength and amplitude interrogation methods are considered as main parameter for analyzing sensing performance of the PCF SPR sensors. To enhance the sensitivity of the sensor, the plasmonic metal layer is required to be coated for improving the interaction of the evanescent field and surface free electrons. Easy interaction with the free electrons of metal layer provides strong coupling between the core guided and SPP mode which enhances the sensor performance.

2.4. Optical properties and metallic films

Gold, silver, copper and aluminum are widely used as the main materials used in SPR sensing [93]. Generally, metals are oxidized due to presence of aqueous environment, water, and humidity. Gold and silver are comprehensively used as a plasmonic material. Gold exhibits strong stability in aqueous environment as well as providing larger shift at resonance peak. However, it shows the broaden resonance peak which may give the false positive analyte detection which diminishes the performance of the sensor [48]. On the other hand, silver shows a narrow-band resonance peak. It is utmost conductive and its optical losses are less among other metals. However, the oxidation of silver in aqueous environment reduces sensing performance [94]. The oxidation process can be inhibited by depositing a thin bimetallic layer on top of the silver surface but it would reduce the sensing performance [95,96]. Recently, it was shown by various studies that graphene can be coated on top of silver to protect silver layer. Graphene is mechanically strong, chemically inert and having hexagonal lattice structure

which prevents oxidation [97–102]. Furthermore, due to π-π stacking, graphene coating with metal surface can enhance the sensing performance. It increases the absorption of analytes owing to the high surface to volume ratio results in improvement of the sensing performance [103–105]. Copper damping rate is the same as gold, and its interband transition is close to gold [106]. Recently, copper-graphene coated plasmonic property has shown long-term durability and stable plasmonic performance (over a year) [97]. In contrast, aluminum as the plasmonic material, has not received much attention for sensing applications as its damping rate and optical losses are high [106]. Furthermore, Al interband transition losses are high in visible range, where the Cu interband transition losses are less and comparable with gold for the wavelengths in the range of 600–750 nm [97]. Moreover, Al shows a broaden resonance peak compared to gold and silver [107]. On the contrary, a sharp and narrow LSPR peak can be achieved by Oxide-free copper [108]. Besides, the novel plasmonic materials, metal oxides contacts such as indium tin oxide (ITO) recently have gained attention in SPR sensing [47]. Its bulk plasma frequency is less than 3 eV, which is smaller compared to gold and silver. ITO layer damping rate is almost as same as gold and silver [109,110].

3. Overview of PCF SPR sensors

One of the SPR sensors limitations is the requirement of having a metallic layer. In PCF SPR sensors, this would cause complexity in fabrication. To simplify the process of depositing metallic layer inside or outside the fiber structure, various designs of PCF SPR sensors have been reported. PCF SPR sensors are classified as internally and externally metal film coated sensors.

3.1. Internally metal film coated PCF SPR sensors

In 2006, MOF based SPR sensors have been reported by Hassani et al. [40]. A two ring, hexagonal PCF structure was proposed where gold layers and liquid were infiltrated selectively in the 2nd ring (Fig. 3a). A small central air-hole was considered for phase matching purpose. Due to different guided modes, three resonance peaks were observed in this design. The 1st resonance peak showed the highest resonance depth with a sensor resolution of 3×10^{-5} RIU (detection of 1% transmitted intensity is assumed). To date, several PCF SPR sensors have been reported where the plasmonic metal layer were coated selectively inside the micron scale air-hole surface [43,44,46,47,59,111–115]. In order to enhance the phase matching between the core-mode and plasmonic mode and also to improve the detection resolution. Selectively silver coated and liquid-analyte filled modelled PCF SPR sensor has been demonstrated (Fig. 3b(i)) [46]. This study shows that the selectively silver layer coating inside the air-holes enhances the performance as compared to the case where internal layer is entirely coated. Due to use of silver layer, sharper peak was achieved which improved the signal-to-noise (SNR) ratio and increased the detection accuracy. Fig. 3b(ii), shows the electric field distribution for analyte RI 1.46. A sharp resonance peak can be observed at 1040 nm wavelength with propagation loss of 108 dB/cm where the core mode and SPP mode affecting the n_{eff} of core guided mode and SPP mode also altered dramatically as shown in Fig. 3b(iii). By measuring the shift in resonance peak, the analyte can be detected.

The sensor's sensitivity is obtained by measuring this shift. Propagation loss also is an important parameter for the practical implementation of the sensor. However, for experimental implementation of PCF SPR sensors, only a centimetre or millimetre length fiber is required to generate the measureable signal. To show a positive and negative refractive index sensor, a liquid-core based PCF SPR sensors have been studied [44,112]. Six selective liquid-analyte filled core has been shown with a metallic channel to simultaneously exhibit the positive and negative RI sensitivity [44]. A maximum positive RI sensitivity of 3600 nm/RIU in the operating range of 1.45–1.46, and a negative RI sensitivity of −5500 nm/RIU have been achieved in the operating range of 1.50–1.53. These sensors have great potential in high refractive index analyte detection. Selectively gold layer coating with liquid-core feature also has potential applications in positive and negative refractive index sensing (Fig. 3c). This configuration diminishes the electromagnetic interference between the cores. The minimum loss value of 80 dB/cm at analyte RI 1.485 was achieved for this sensor. A theoretical study shows that the polymer based PCF SPR biosensors incorporating indium tin oxide (ITO) allows the utilization of SPR [47]. ITO enables sensing operation to be extended into telecommunication applications, where light launching is feasible and the confinement loss is less compared to the visible range. Moreover, plasmonic resonance can be tuned by modifying the thickness or intrinsic properties of ITO which has a broad transparency range. In addition, to operate the sensing operation in near-infrared (IR) region, high refractive index of titanium dioxide (TiO_2) based PCF SPR sensor have been studied (Fig. 3d) [111]. Gold-TiO_2 and liquid are infiltrated inside the air-holes to improve SPR sensing performance. Gold-TiO_2 and liquid are infiltrated inside the air-holes to improve SPR sensing performance. The numerical analysis showed that the loss spectrum could be tuned by changing the gold and TiO_2 thickness. It exhibited the minimum loss value of 58 dB/cm while analyte RI 1.335.

However, selective coating of thin metal film inside the micro air-holes is sophisticated process from fabrication point of view. This limits the practical implementation of PCF SPR sensors. To eliminate the thin film coating, nanowire based PCF SPR sensors have been reported [56,116–118]. A silver nanowire based PCF SPR sensor has been reported for the RI detection, where the nanowires and liquid were selectively filled 1st ring of the PCF [116]. It showed the maximum loss of 2200 dB/m at analyte RI 1.33 and achieved the maximum sensor resolution of 5×10^{-5} RIU. Placing the silver nanowires in the 2nd ring reduces the transmission loss which allows fiber length of 2–3 cm to observe the SPR sensing. Recently, by using the silver nanowires in the 1st ring of PCFs, a sensor for temperature measurement is demonstrated (Fig. 3e) [117]. Blue shift occurred due to the increase in temperature with a sensitivity of 2.7 nm/°C. Hollow-core PCF has been experimentally developed for the RI detection, where the core is filled with liquid and silver nanowires (Fig. 3f) [118], resulting in wavelength sensitivity of 14,240 nm/RIU. Furthermore, hollow-core photonic band gap fiber (HC-PBGF) based SPR sensor was numerically investigated where the core was filled with liquid and silver nanowires (Fig. 3g) [119]. The sensor was able to detect RI lower than 1.26 and the maximum sensitivity was achieved at 2151 nm/RIU. Nanowire-based sensing fiber could be realized by incorporating the Tylor wire procedure with the Stack-and-Draw fiber drawing method [67]. Nevertheless, self-calibration with a known analyte as well as change of the analyte sample inside the air-holes are considered as experimental challenges. Moreover, selective liquid infiltration and insertion of silver nanowires of micro air-holes would also be complicated task. Placing the metal layer/nanowires in vicinity of the core, results in attraction of the fields towards the metal/nanowire surface causing large loss. This loss inhibits the practical realization of PCF SPR sensor. The input light will be disappeared immediately after it has been lunched. It is not possible to generate a measurable signal at the output for detection of the sample. High fiber loss limits the fiber length. In general, shorter fiber length is desirable as by increasing its length the loss is increased. Due to small length of sample PCF, it is required to align or splice it with the normal single mode fiber (SMF) to implement it experimentally.

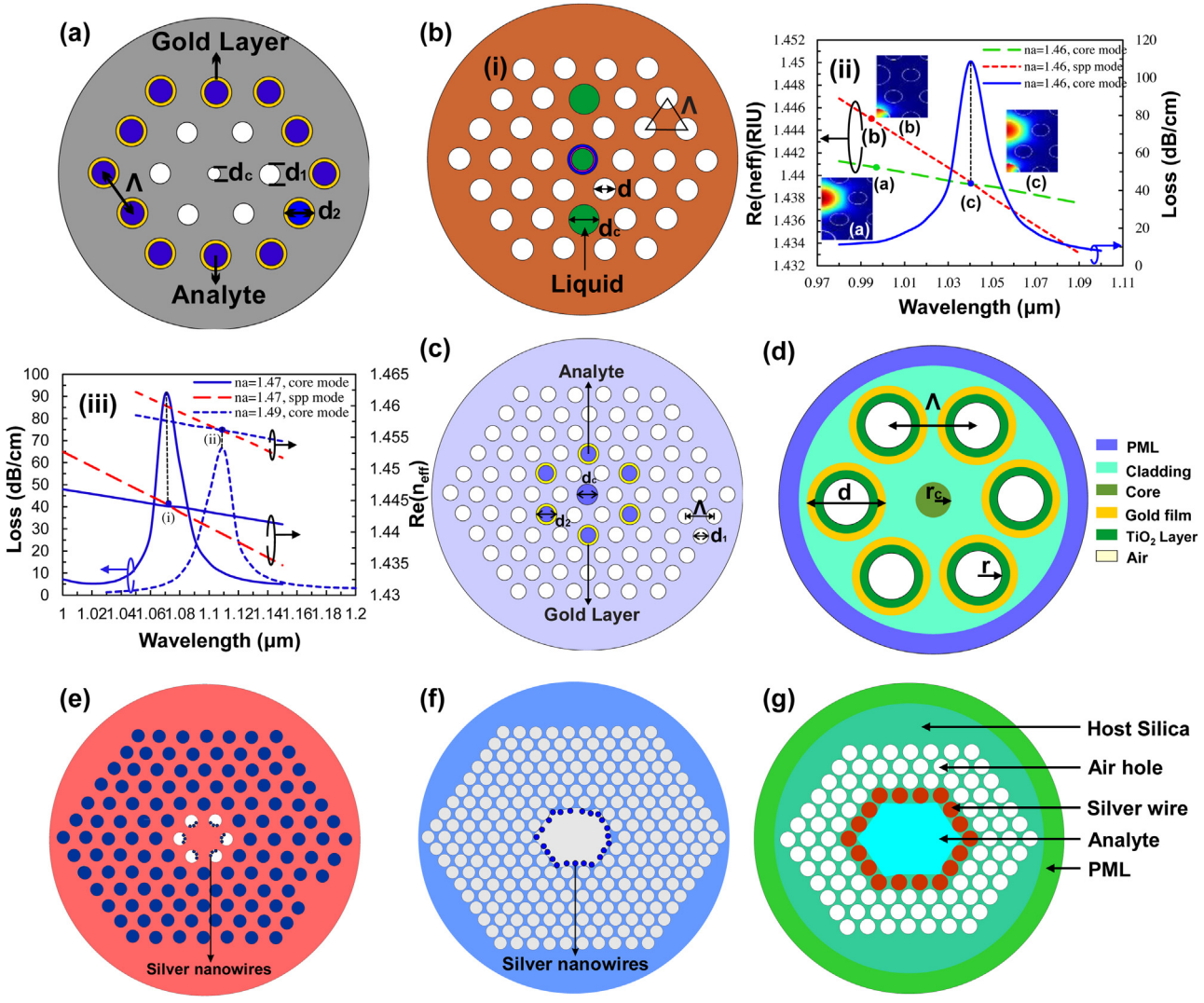

Fig. 3. Inside metal coating based PCF SPR sensors. (a) Gold coated in the 2nd ring ($d_c = 0.45\Lambda$, $d_1 = 0.6\Lambda$, $d_2 = 0.8\Lambda$, $\Lambda = 2\,\mu m$ and gold layer thickness = 40 nm). (b) (i) Selectively silver deposited core ($d_c = 0.8\Lambda$, $d_1 = 0.6\Lambda$, $d_2 = 0.8\Lambda$, $\Lambda = 2\,\mu m$ and silver layer thickness = 40 nm), (ii) field distribution with phase matching phenomena, and (iii) phase matching phenomena shifted with varying analyte RI. (c) Selectively gold-coated with liquid-filled core ($d_c = 0.8\Lambda$, $d_1 = 0.5\Lambda$, $d_2 = 0.8\Lambda$, $\Lambda = 2\,\mu m$ and gold layer thickness, t = 40 nm). (d) Multiple holes coated with gold-TiO_2 layer ($r_c = 3.5\,\mu m$, $r = 6\,\mu m$, $\Lambda = 13\,\mu m$, gold layer thickness = 30 nm and TiO_2 layer thickness = 75 nm). (e) Liquid and silver nanowire filled temperature sensor. (f) Hollow-core filled with liquid and silver nanowires and (g) Silver-wire filled HC-PBGF.

Table 2
Performance analyses of internally coated PCF SPR sensors.

Characteristics	Wavelength (nm)	RI Range	Interrogation	Sensitivity	Resolution (RIU)	Ref.
Solid-core honeycomb fiber	940–1040	1.320–1.322	Wavelength	13,750 nm/RIU	7×10^{-6}	[41]
			Amplitude	400 RIU^{-1}	2.5×10^{-5}	
Small solid-core based Bragg fiber	780–920	1.325–1.326	Wavelength	12,000 nm/RIU	8.3×10^{-6}	[42]
			Amplitude	269 RIU^{-1}	3.7×10^{-5}	
Selectively liquid-filled core	900–1200	1.45–1.53	Wavelength	−5000 nm/RIU	2.7×10^{-6}	[44]
Silver-graphene deposited core	970–1200	1.46–1.49	Wavelength	3000 nm/RIU	3.3×10^{-5}	[46]
			Amplitude	418 RIU^{-1}	2.4×10^{-5}	
Selectively ITO coated polymer PCF	1275–1690	1.33–1.35	Wavelength	2000 nm/RIU	5×10^{-5}	[47]
Selectively filled silver nanowires	400–1400	1.330–1.335	Wavelength	N/A	4.5×10^{-5}	[52]
			Amplitude	203 RIU^{-1}	4.9×10^{-5}	
Multi-hole fiber based SPR sensor	1340–1460	1.33–1.35	Wavelength	2000 nm/RIU	5×10^{-5}	[111]
			Amplitude	370 RIU^{-1}	2.7×10^{-5}	
Selectively gold coated with liquid-filled core	850–1400	1.460–1.485	Wavelength	−4,354.3; 2280 nm/RIU	N/A	[112]
Selectively gold coated fiber	500–850	1.37–1.41	Wavelength	5500 nm/RIU	N/A	[114]
Hollow-core filled with silver-nanowires	560–610	1.1–1.6	Wavelength	14,240 nm/RIU	N/A	[118]
Multi-core holey fiber	400–1800	1.43–1.53	Wavelength	9,231.2 nm/RIU	N/A	[120]

Table 2 shows the performance comparisons of the internally coated (metal and nanowire) PCF SPR sensors.

3.2. Externally coated metallic film PCF SPR sensors

To overcome the metal coating and liquid-analyte infiltration inside the air-holes, externally coated PCF SPR sensing approaches have been proposed. Metal layer and sensing medium were placed on the outer side of the fiber structure which makes the sensing mechanism more convenient. Based on the sensor structures and applications, external sensor approaches can be classified in the following three categories: D-shaped PCF SPR sensors, slotted PCF SPR sensors, and improved external approach of PCF SPR sensors.

3.2.1. D-Shaped modeled PCF SPR sensors

D-shaped PCF have attained attention for SPR sensing where top of the fiber cladding is polished to be flat. PCFs with polished part of cladding resemble D-shape where the metal layer and sample are placed on top of the flat part. In D-type PCF, metallic layer can be placed near to the core which facilitate the strong interaction with sample, leading to enhancement of the sensing performance. To date, several D-shaped PCF SPR sensors have been reported [45,50,57,121–125]. Examples of D-shaped PCF SPR sensor are shown in Fig. 4a [45]. The solid core was used with scaled down air holes in the 1st ring, and thin gold layer was deposited on top of the flat part. By modification of D-shape PCF SPR sensors geometry, their output can be altered. For instance, by increasing the polishing depth, resonant wavelength would be tuned from red shift to blue shift. Due to increasing the polishing depth, metal surface approaches towards the core and therefore a strong coupling occurs between the core mode and analyte. The achieved sensor sensitivity was 7300 nm/RIU and the figure of merits of 216. Numerical simulation of hollow-core D-shaped PCF SPR sensor was also reported [121]. A high refractive index liquid (RI = 1.39) mixer was used in the hollow core, having the sensitivity of 6430 nm/RIU in the operating range of 1.33-1.34. It shows the maximum imaginary $n_{eff} = 2.5 \times 10^{-5}$ which indicates the approximate loss of 19.9 dB/cm at the wavelength of 684.6 nm. Recently, a D-shaped PCF SPR sensor has been reported for the biosensing application, where a graphene-silver combination was used (Fig. 4b) [122].

In order to enhance the sensing performance, two large air holes were milled along the central hole to introduce birefringence. Rest of the air-holes in the 1st ring were scaled down to create a large gap for improving the coupling between core and SPP modes. The phase matching parameters such as n_{eff} of core and spp mode are matched at 480 nm wavelength and a sharp loss peak was observed (Fig. 4c). Solid-core D-shaped PCF with resolution of 9.8×10^{-6} RIU were demonstrated by Santos et al. [123]. The primary ring in air-holes was omitted in the upper side for enhancing the excitation in metal surface. As a result of excluding the air-holes, the maximum loss of 70 dB/mm at 650 nm wavelength with analyte RI 1.36 was exhibited. Conventional D-type optical fiber based SPR sensors performance were compared to microstructured D-shape fiber. The sensor shown the sensitivity of 2.8×10^3 to 10×10^3 nm/RIU and a resolution from 3.6×10^{-5} to 9.8×10^{-6} RIU. D-shaped hollow-core MOF based SPR sensor has been demonstrated by Luan et al. [124]. In this design, the sensor core is scaled down in order to establish and tune the phase matching between the core and SPP mode (Fig. 4d). Increasing the core diameter enhances the resonance peak shift and produces higher propagation loss to increase the sensitivity with respect to wavelength and amplitude interrogation methods. On the other hand, increasing the core diameter would decrease the phase difference of two modes resulting in lower phase sensitivity. By excluding the upper side air-holes in the 1st ring, large confinement loss of 1700 dB/cm at 675 nm wavelength was achieved. It was shown that the maximum phase shift of 503 deg/cm at 676 nm wavelength and maximum phase sensitivity of 503,00 deg/RIU/cm can be achieved (Fig. 4e). Recently, rectangular lattice based D-shaped PCF SPR sensor is demonstrated in Fig. 4f [50]. In vicinity of the solid-core, two large air holes are positioned close to the solid-core in order to enhance the sensing performance of the figure of merit 478.3 RIU^{-1}, which is the highest sensitivity FOM among the reported PCF sensors to date.

Although D-shaped PCF SPR sensor overcame uniform coating issues but there are reported D-shaped structures in which showing large confinement loss due to the sealed upper air holes [123,124]. However, to control the propagation loss, D-type fiber structure is suitable as its core is surrounded with several rings and only the upper side is required to be etched/polished to make D-shape. However, these required accurate polishing of the sensor surface to specifically eliminate a prearranged structure of the PCF.

3.2.2. Slotted based modeled PCF SPR sensors

For the detection of multiple analytes, slotted PCF SPR sensors have been developed by various studies [54,58,97,126–128]. By tailoring the air hole diameter in the first ring, birefringent effects could be realized. Birefringent behavior led to the stronger light propagation in x and y polarization for the detection of multiplexed analytes. Slotted PCF SPR sensors were demonstrated for the detection of biolayer configuration by Hassani (Fig. 5a) [126]. Gold layer and biolayer were placed outside the fiber structure. Three small air holes were placed near to the gold surface. Changing the diameter of these holes enables tuning the plasmonic behavior. This sensor also has potential application in monitoring the concentration of nanoparticles in photodynamic cancer therapy [129]. It exhibits the propagation loss of 97 dB/cm while analyte RI = 1.33 and biolayer RI = 1.42. It shows the changes of biolayer thickness up to 10 nm results in shifting peak wavelength by 23 nm (Fig. 5b). Two microfluidic slots with a single ring based PCF SPR sensor was proposed, where the air-holes were scaled down selectively to control the light propagation track (Fig. 5c) [130]. Miniature air holes create the gap which helps the penetration of the evanescent field into the metal surface. It was shown that the maximum wavelength interrogation sensitivity of 4000 nm/RIU can be achieved. The minimum loss of 140 dB/cm at 635 nm wavelength while analyte RI = 1.33 was illustrated. A theoretical study for configuration of four metalized microfluidic slots based on a PCF SPR sensor has been reported [127]. In this sensor, scaled down circular air-holes were used in vicinity of central hole to penetrate the light along these side layers for efficient excitation of surface plasmon.

Elliptical orientations of air-holes were placed in other sides to control the direction of light propagation. Since the elliptical surface is broader compared to the circular one, the propagation in certain directions are enhanced. According to the wavelength interrogation method, the sensor resolution was reported to be 4×10^{-5} RIU and 8×10^{-5} RIU for $HE11x$and$HE11y$, respectively. Different analytes can flow through the four different microfluidic slots for multiplexed analyte detection. Recently, a birefringent PCF with two microfluidic slot based SPR biosensors has been studied (Fig. 5d) [128]. Birefringent behavior was introduced by placing the air holes in the vicinity of the central air hole. This makes stronger coupling between the x- or y-polarization of core mode and spp mode results in improving the sensor performance. The resolution of 5×10^{-5} RIU and 6×10^{-5} RIU for x and y polarization, respectively was achieved. The numerical study of entirely elliptical air hole based PCF SPR biosensor has been presented, where the four microfluidic channels were coated with gold layer (Fig. 5e) [54]. Tantalum pent-oxide (Ta_2O_5) metallic layer which has broad range of transparent spectrum was deposited on the gold surface. As a result of having the metallic layer, the concentration of nanoparticles can be studied. A small central circular air hole was considered to tune the phase matching phenomena. This sensor

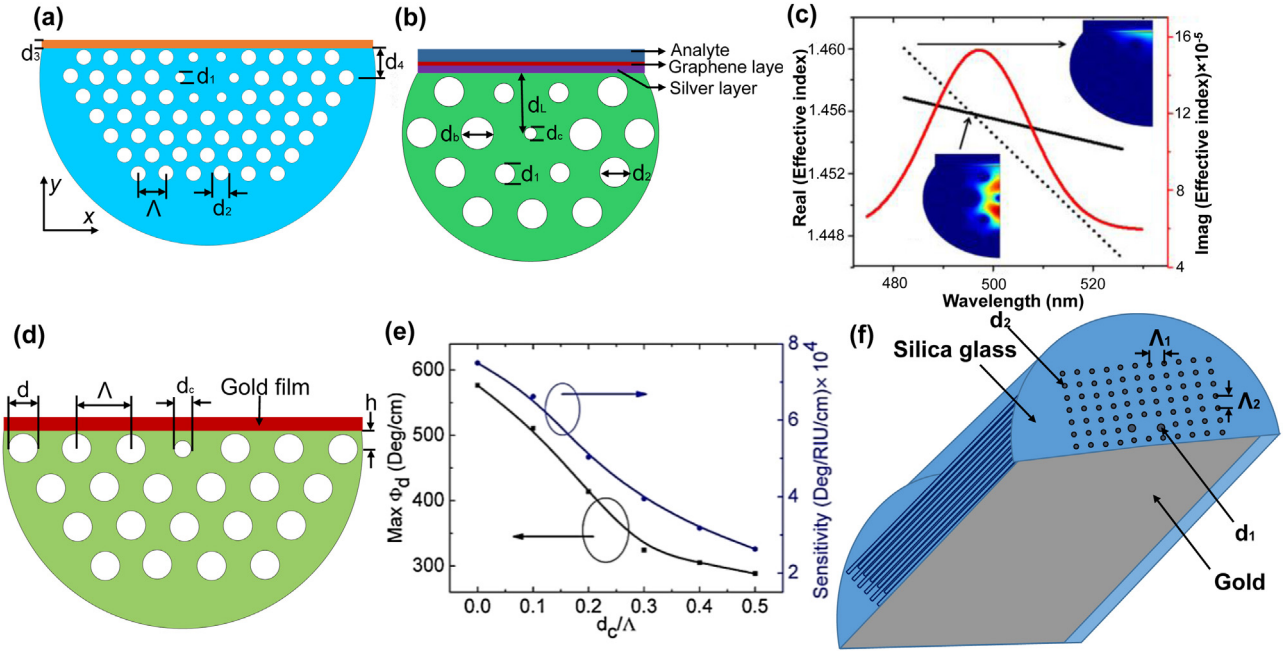

Fig. 4. Modeled D-shaped PCF SPR sensors. (a) Solid core with scaled down air-holes in the 1st ring ($d_1 = 0.6\Lambda$, $d_2 = 0.8\Lambda$, $d_3 = 40$ nm, $d_4 = 2.66$ μm and $\Lambda = 2$ μm). (b) Graphene-silver coated scaled down air-holes in the 1st ring ($d_c = 0.5$ μm, $d_1 = 0.6$ μm, $d_2 = 1.4$ μm, $d_b = 1.4$ μm and $d_L = 2.7$ μm). (c) Field distribution and phase matching phenomena. (d) Scaled down hollow-core ($d_c = 0.2\Lambda$, $d = 0.8$ μm, $\Lambda = 2$ μm, $h = 0.45\Lambda$ and gold film thickness = 40 nm). (e) Maximum phase difference and phase sensitivity with varying pitch while $n_a = 1.33$ and (f) Solid-core with rectangular lattice ($d_1 = 1.2\Lambda_2$, $d_2 = 0.75$ μm, $\Lambda_1 = 2$ μm, $\Lambda_2 = 1.5$ μm and gold layer thickness = 40 nm).

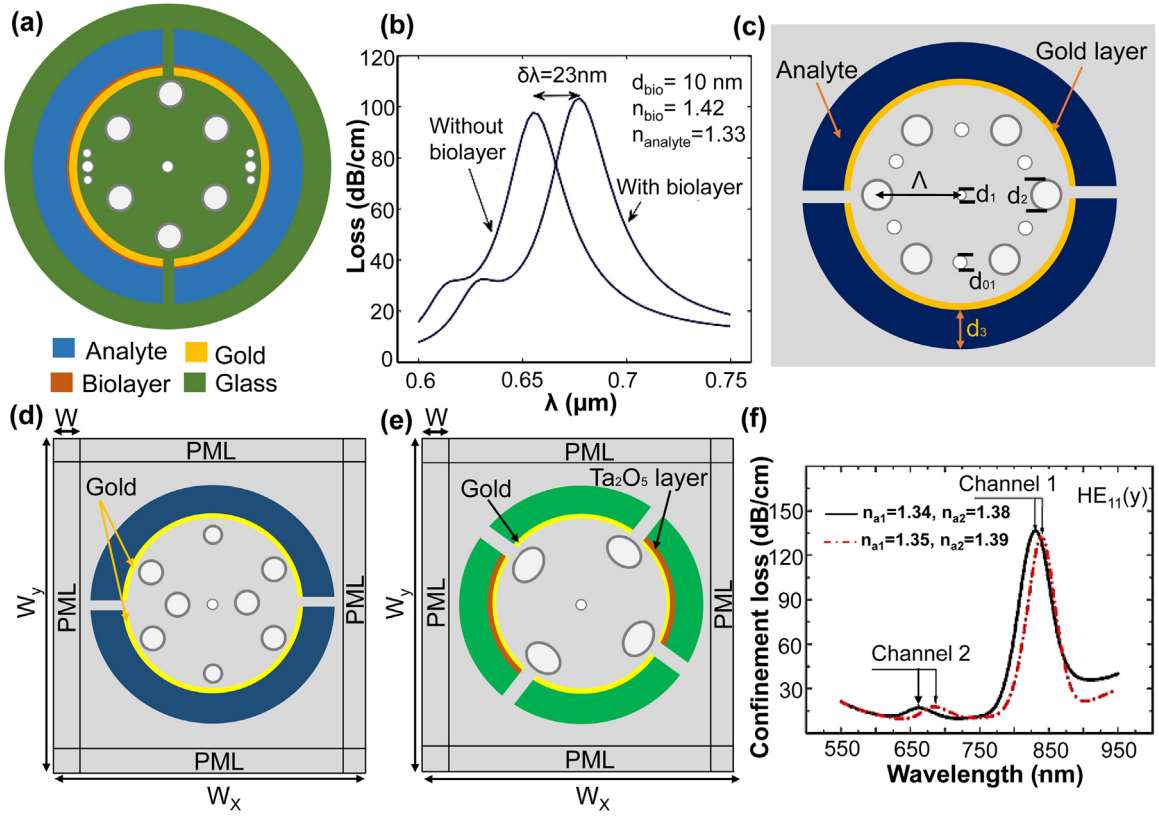

Fig. 5. PCF SPR sensors for multiplexed analyte detection. (a) Two microfluidic slots with gold biolayer. (b) Loss spectrum with varying biolayer thinkness. (c) Two micro fluidic slots with a single ring ($d_{01} = 0.15\Lambda$, $d_1 = 0.2\Lambda$, $d_2 = 0.35\Lambda$, $d_3 = 1.5$ μm, $\Lambda = 1.5$ μm and gold layer thickness = 40 nm). (d) Two microfluidic slots with irregular air-holes (gold layer thickness = 40 nm). (e) Four micro-fluidic slots with gold-Ta_2O_5 layer, and **(f)** Loss spectrum for multi-analyte detection.

showed the wavelength sensitivity of 4600 nm/RIU. Also the capability of detecting multi-analyte was investigated. It compromised of two different channels with different refractive index n_{a1} and n_{a2} and the mode coupling between core mode and spp mode among the channels was observed (Fig. 5f). Nevertheless, elliptical air-hole based PCF fabrication is still in progress. Fabrication of the microflu-

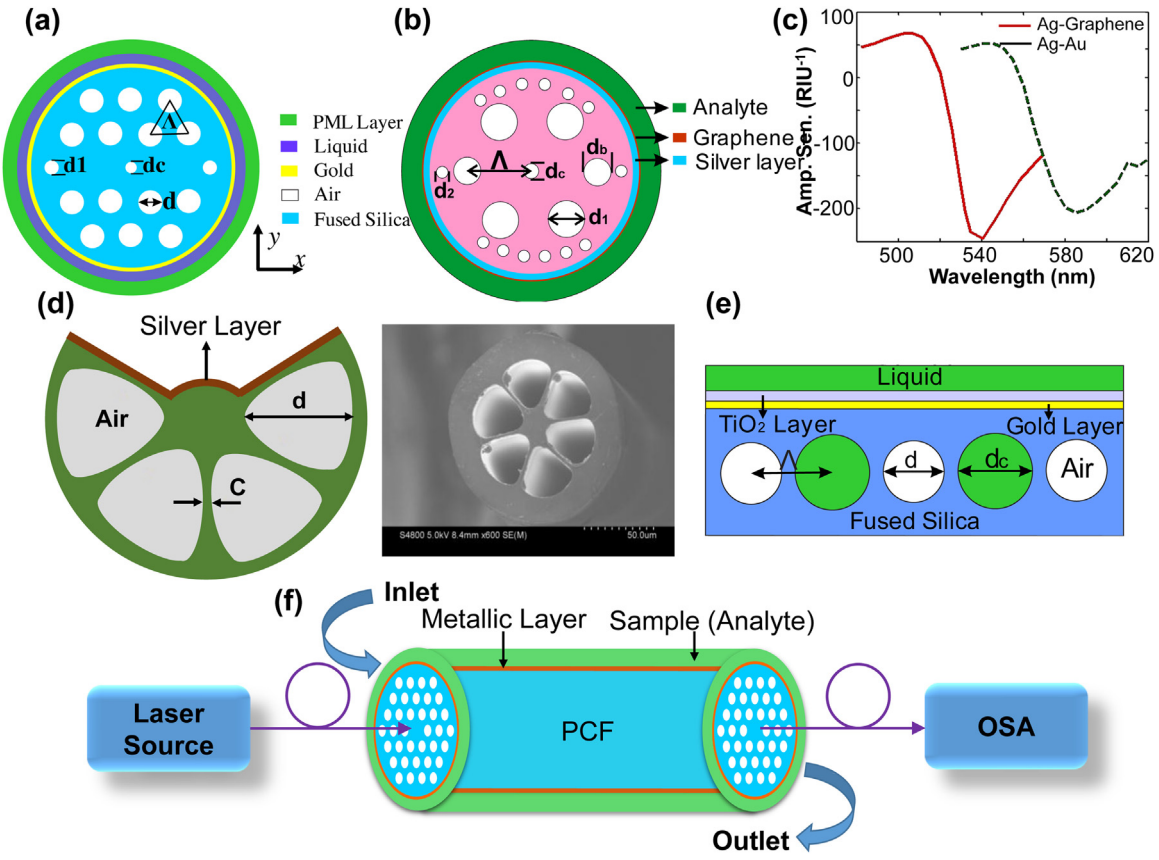

Fig. 6. PCF SPR sensor featuring external sensing approach. (a) Two sealed air holes beside the central air hole ($d = 0.5\Lambda$, $d_c = 0.15\Lambda$, $d_1 = 0.25\Lambda$, and $\Lambda = 2\,\mu m$ and gold layer thickness = 40 nm). (b) Selectively placed air holes in the 2nd ring ($d_c = 0.3\Lambda$, $d_1 = 0.6\Lambda$, $d_2 = 0.2\Lambda$, $d_b = 0.4\Lambda$, $\Lambda = 2\,\mu m$, graphene layer = 0.34 nm and silver layer = 30 nm). (c) Amplitude sensitivity comparison of silver and gold coated with graphene. (d) Exposed-core grapefruit fiber ($d = 80\,\mu m$, $c = 2\,\mu m$ and silver layer thickness = 40 nm), Reprinted with permission from Ref [131]. Copyright 2015, Multidisciplinary Digital Publishing Institute. (e) Photonic crystal flat fiber ($d = 0.5\Lambda$, $d_c = 0.15\Lambda$ and $\Lambda = 2\,\mu m$, TiO_2 thickness = 70 nm, and gold layer thickness = 40 nm), and (f) Schematic diagram of the experimental setup.

idic channels are also challenging process. However, placing the metallic and sensing layer outside the fiber structure provide can cause less complexity in fabrication. Single ring PCFs exhibit high confinement loss but the loss can be reduced by increasing the number of rings.

3.2.3. *Improved external approach of PCF SPR sensors*

The PCF SPR sensors are improved by placing a metal layer and sensing medium outside the fiber structure [33,40,41,48,131–135]. Hassani et al. reported two large semi-circular gold and sample layers placed outside the fiber structure [40]. Due to requirement of thin semi-circular structure, practical realization of this design is difficult. To simplify the fabrication process, Popescu et al. [134] used single circular gold and sample layers outside the fiber structure which facilitates simplified fabrication process as well as simple sensing process. The influence of air-hole sizes in the 1st ring of the microstructured fiber on the plasmonic phenomena has also been investigated. The maximum amplitude sensitivity and the sensor resolution were found to be 3941.5 RIU^{-1} and 1×10^{-5} RIU, respectively [135]. A simple configuration for PCF SPR biosensors have been reported, where the air holes in the vicinity of central hole were sealed and in the same row, air holes were scaled down to create a gap for the penetration of evanescent fields to excite the surface plasmons (Fig. 6a) [49]. The maximum wavelength and amplitude sensitivity were 4000 nm/RIU and 320 RIU^{-1}, respectively. Moreover, the confinement loss value of 17 dB/cm at 1.33 analyte RI was achieved. Due to surrounding the core by air holes, lower loss value was observed found for this arrangement. A novel microstructure fiber based SPR sensor has been reported which exhibits two types of core-guided mode based on analyte RI variation [136]. At analyte RI 1.36 SPR sensor showed the better response for type II core with the sensitivity of 405.6 RIU^{-1} which is comparable with ref. [49]. It has been shown that the response of the proposed SPR sensor has a maximum wavelength and amplitude sensitivity of 7000 nm/RIU and 886.9 RIU^{-1}, respectively for analyte RI 1.39. Birefringent effects with graphene-silver combination were also studied to enhance the sensitivity due to the large surface to volume ratio (Fig. 6b) [48]. In this sensor, light propagation in a specific direction is controlled by selectively placing the small air holes in the 2nd rings. The maximum amplitude sensitivity was 860 RIU^{-1} with a sensor resolution of 4×10^{-5} RIU (assuming minimum 1% transmitted intensity could be detected). It exhibits the minimum confinement loss of 190 dB/cm at 510 nm wavelength while analyte RI = 1.33. It was also found that the silver with graphene has 18% higher amplitude sensitivity as compared to god coated silver (Fig. 6c). Another external approach involved placing two cores near the metal layer which enhance the coupling of core-guided mode and SPP mode [133]. Only one core could be able to detect the sample. The second core is used in order to increase the detection area. The sensor sensitivity of 1000 nm/RIU and resolution of 1×10^{-4} RIU were achieved. It was observed that the minimum loss value was 85 dB/cm at 690 nm wavelength. An exposed-core grapefruit fiber SPR biosensor was reported by Yang et al. (Fig. 6d) [131]. Grapefruit fibers are easy to fabricate and it is widely available in commercial aspects. In this configuration, the exposed section was coated with a silver layer to realize the generated SPR.

This sensor showed the increased sensitivity for high analyte RI values and had a maximum wavelength interrogation sensitiv-

Table 3
Performance analyses of externally coated PCF SPR sensors.

Characteristics	Wavelength (nm)	RI Range	Interrogation	Sensitivity	Resolution (RIU)	Ref.
Solid core D-shaped fiber	550–800	1.33–1.38	Wavelength	7300 nm/RIU	N/A	[45]
Graphene-silver coated outside fiber structure	475–675	1.33–1.37	Amplitude	860 RIU^{-1}	4×10^{-5}	[48]
Gold coated external sensing approach	500–750	1.33–1.37	Wavelength	4000 nm/RIU	2.5×10^{-5}	[49]
			Amplitude	320 RIU^{-1}	3.1×10^{-5}	
Multichannel PCF	550–950	1.33–1.39	Wavelength	4600 nm/RIU	2×10^{-5}	[54]
Hollow core D-shaped PCF	650–850	1.32–1.36	Wavelength	6430 nm/RIU	N/A	[121]
Graphene based D-shaped fiber	480–650	1.33–1.37	Wavelength	3700 nm/RIU	2.7×10^{-5}	[122]
			Amplitude	216 RIU^{-1}	4.6×10^{-5}	
Scaled down hollow-core D-shaped fiber	550–750	1.33–1.34	Wavelength	2900 nm/RIU	N/A	[124]
			Amplitude	120 RIU^{-1}	N/A	
			Phase	50,300 deg/RIU/cm	N/A	
Four microfluidic slots	500–800	1.33–1.34	Wavelength	N/A	8×10^{-5}	[127]
			Amplitude	N/A	6×10^{-5}	
Two microfluidic slots	500–800	1.33–1.34	Wavelength	N/A	6×10^{-5}	[128]
			Amplitude	N/A	4×10^{-5}	
Exposed-core grapefruit fiber	460–1120	1.33–1.42	Wavelength	13,500 nm/RIU	N/A	[131]
Solid core microstructured optical fiber based SPR sensor	770–850	1.36–1.39	Wavelength	7000 nm/RIU	4×10^{-5}	[136]
			Amplitude	886.9 RIU^{-1}	1.7×10^{-5}	

Table 4
Advantages and disadvantages of different types of PCF SPR sensors.

Classification of PCF SPR sensors	Advantage	Disadvantage	Structural diagram	Ref.
Selectively metal coating	Air-holes act as a cell and sample can flow through the air-holes.	Selectively metal coating is challenging as the air-holes size in micron scale.	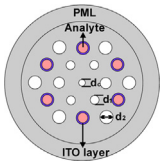	[47]
Internal nanowires filling	Small nanowire portion is required and sample can flow through the air-holes.	Selectively nanowires with liquid filling is challenging.	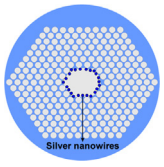	[118]
D-shaped	Sample can flow through the outer surface which make the sensor structure simpler.	Accurate polishing or etching effort is required.		[124]
Micro fluidic slots	Able to detect multiple analyte at the time instant.	Creating the microfluidic slots is challenging.	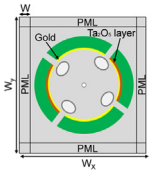	[128]
External sensing approach	Sample can be detected in the external surface of fiber structure.	Irregular air-holes size are required. However, thicker or thinner wall capillary can solve this problem.	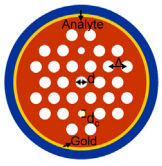	[133]

ity of 13,500 nm/RIU. Multi core flat fiber (MCFF) which is mainly based on photonic crystal has also been modelled for SPR sensing (Fig. 6e) [33]. The main advantage of the MCFF is having high sensitivity compare to other types of SPRs. Also its sensing area can be scalable due to its flat large surface. Additionally, the functionality and flexibility of the proposed structure with having high RI fluids open up many opportunities for designing versatile SPR sensors based on this hybrid format of waveguide. The structure of MCFF combines the advantages of conventional optical fiber with the multi-functionality of planar waveguides. Due to its flat surface, smoother surfaces can be achieved after the deposition of metal. The MCFF SPR sensor showed a maximum wavelength and amplitude interrogation sensitivity of 23,000 nm/RIU and 820 RIU^{-1}, respectively. Outer metal layer enables the detection of an unknown analyte by analyzing the medium passing through the metallic surface.

A schematic of the experimental setup for PCF SPR sensor has been illustrated in Fig. 6f. Beam of light from a laser source is coupled to the circular PCF structure. A circular sample holder was used to embrace the PCF structure. Analyte sample flow was controlled by using a pump and a flow-meter. Finally, the transmitted light is coupled to an optical spectrum analyzer (OSA) to analyses the

output light. The wavelength interrogation method is widely used for PCF SPR sensor. In this method the laser source is irradiated at one end of the fiber and the output (altered peak) will be observed in the OSA which is connected to the other end of fiber. Finally by varying the sample RI, the blue shift or red shift is achieved which is used for detection of analyte.

Table 3 shows the performance comparison of the reported PCF SPR sensors.

Overall, PCFs can be fabricated by following various established methods such as capillary stack and drawing procedure [137], drilling [138], slurry casting [139], sol-gel casting [140], and extrusion method [141]. Among the PCF drawing methods standard stack and drawing procedure is widely used as it enables fabricating the PCF with some impurities in silica capillaries and provide the minimum transmission loss of 0.18 dB/km at 1.55 μm wavelength [142]. However, complexity in PCF structures is one of the common difficulties observed in most of the SPR sensors. To control the light propagation for optimizing the SPR performance, air holes geometries can be optimized. The fabrication of asymmetrical PCF structures where the different diameters of air holes are needed is challenging process. Thus, simpler and scalable structures will allow ubiquitous remote SPR sensing. However, requiring metal coating on circular surface of PCFs is of the major issues which prevents the practical realization of PCF SPR sensor. Normal metal coating methods such as RF sputtering, thermal evaporation methods, electroless plating and wet-chemistry deposition creates the massive surface roughness in coating the circular surface. Chemical vapor deposition (CVD) method also reported as a possible coating method in a circular surface, although it involves complex organometallic chemistry [143,144]. Furthermore, Tollens reaction is an alternative approach for metal coatings in circular surfaces such as external layer of optical fiber or inner air holes surfaces [145,146]. The chemical process is more cost effective and practical compared to other stated methods. In order to characterize and utilizing the sensor the self-calibration procedure is required. Sample liquid can be exchanged by using the water or pumping the nitrogen through the fiber [145]. Furthermore, the problem of large confinement loss in PCFs also can be controlled by optimizing the air holes geometry and increasing the number of rings.

4. Potential future directions

PCF SPR sensing is a promising and competitive sensing technology. However, at the device development front, PCF SPR sensors are still at the early stage. Most of the studies reported in the literature involve proof of concept demonstrations, theoretical and computational models. The application of established theoretical models to sensor implementation is limited because of fabrication challenges. Although some experimental devices reported in the literature, their applications are found in limited research domain [117,118]. Therefore, the empirical performances of the modelled sensors are still not fully investigated. Potential future work should focus on (i) proof of concept demonstration to real PCF SPR sensor development and (ii) detection of analytes for wider range of chemical and biological samples. One possible development direction for the PCF SPR sensors is portable and rapid lab-on-a-chip assays for point-of-care diagnostics. The objective could be to replace current adopted fluorescence detection with label-free PCF SPR sensing, which may improve the ability to sense different types of analytes, decrease test costs, and save time by reducing sample preparation process. In contrast to fluorescent sensors, the PCF SPR may be configured to be reusable for incessant monitoring applications. Therefore, PCF SPR sensor structures should be fabricated by using simple and cost effective method. To date, different structures comprising of inner or outer metal coatings have proposed. Most of the reported structures are complex, which limits the device implementation. The D-shaped and the external sensing approach of PCF SPR sensor might be an alternative way to reduce the fabrication complexity [45,48,49,54,122,124]. However, for these approaches, the air-holes in the PCF are no longer useful as microfluidic channels are used for the sensing applications. Another main limitation of PCF SPR sensor implantation is the thin selective metal coating. Recently, there are few designs of PCF SPR sensors which have been fabricated for the purpose of temperature measurement and chemical sensing [117,118]. However, their applications are again limited by fabricating uniform and selective metal coating. A uniform metal nanolayer in the capillaries is vital. Uniform metal layer reduces surface roughness, which will ensure laminar analyte flow for improved sensing performance. Uniform nanolayer coating can be achieved by CVD. Metal nanoparticles may also be implemented by controlling their size during fabrication to form a thin and uniform coating in the PCF. Quite few studies been done on metal nanoparticle-modified PCF in Surface-Enhanced Raman Scattering (SERS) [147–150]. Moreover, SPR-like sensing using surface waves is not exclusive for the visible-near-IR spectral ranges. Similar sensors can be built at lower frequencies (mid-IR and THz) by replacing metals with polaritonic materials and polaritons instead of plasmons [151]. Although silica based PCFs are not able to perform in THz region but, polymers such as low-density polyethylene (LDPE), polyamide-6 (PA6), polytetrafluoroethylene (PTFE or Teflon®) and cyclic olefin/ethylene copolymer (TOPAS®) can be used as a background material for this region [152,153]. However, among these polymers TOPAS is widely used due to its negligible absorption and broad range of constant refractive index value.

Another experimental challenge in utilizing the PCF SPR sensors is controlling the directions of light propagation and flow of the sample. To fill the microfluidic channels of the PCF with a sample during sensing, the solution will be required to be passed through the PCF in the same direction as the light propagation. The filling of fluid will require the displacement of MOFs from the setup. Moreover, the re-alignment of the PCF may affect the coupling condition. When the accuracy of measurements is crucial, altering the coupling condition may cause inaccurate results. This problem could be solved by constructing an external microfluidic channel. Most of the PCF SPR sensors are based on inner microfluidic channels for the flow of analytes. The fabrication of an external microfluidic channel will also reduce fabrication complexity. For example, an external fluidic jig could be introduced to a D-shaped or outside the PCF structure to create a sealed microfluidic system, so that the exchange of solution can occur on the surface of the metal coating. This ensured device simplicity and reasonable performance can be achieved. These devices could be multiplexed to quantify different analytes simultaneously.

5. Conclusions

Proof of concepts are mainly demonstrated by theoretical and computational modelling by using finite element analysis. Numerical and analytical investigations of PCF SPR sensors have shown their capability in providing high sensitivity with respect to small RI changes in external stimuli.

The summary of above discussed reported PCF SPR sensors along with their advantages and disadvantages are shown in Table 4.

Regular PCF structures for SPR sensing could be fabricated by standard stack-and-draw fiber drawing method combined with external coatings to reduce the complexity in fabrication. One of the main issues of PCF SPR sensor is surface roughness of the coated metal inside or outside the circular surface structures. PCF SPR sensors offer high-sensitivity and compactness for the quantifications of analyte concentrations in real time measurements. The avail-

ability of the holes in the PCF allows configuration of microfluidic channels for sensing applications. As compared to the conventional prism-based SPR sensors, the experimental setup for a PCF SPR sensor is relatively simple, and does not require highly-skilled personnel for performing the measurements. Moreover, the PCF SPR sensors show a promising ability in the detection of various types of chemical and biological analytes. The performance of the PCF SPR biosensor technology will evolve with advances in PCF fabrication and metal nanoparticle syntheses. In future by advances in fabrication techniques, the PCF SPR sensors can be utilized in various applications ranging from medical diagnostics, biochemical, environmental monitoring, and food safety to security.

Author contributions

A.A.R. and R.A. designed the project, collected the data and wrote the article. A.K.Y., H.B., A.S., G.A.M., S.H.Y. and F.R.M.A. made intellectual contributions and edited the article. Authors thank Dr. Wei Ru Wong for discussions.

Acknowledgement

This work is supported by the University of Malaya MOHE-High Impact Research grantUM.0000005/HIR.C1.

Appendix A. Supplementary data

Supplementary data associated with this article can be found, in the online version, at http://dx.doi.org/10.1016/j.snb.2016.11.113.

References

[1] A. Nooke, U. Beck, A. Hertwig, A. Krause, H. Krüger, V. Lohse, et al., On the application of gold based SPR sensors for the detection of hazardous gases, Sens. Actuators B 149 (2010) 194–198.
[2] J. Homola, J. Dostalek, S. Chen, A. Rasooly, S. Jiang, S.S. Yee, Spectral surface plasmon resonance biosensor for detection of staphylococcal enterotoxin B in milk, Int. J. Food Microbiol. 75 (2002) 61–69.
[3] V. Koubova, E. Brynda, L. Karasova, J. Škvor, J. Homola, J. Dostalek, et al., Detection of foodborne pathogens using surface plasmon resonance biosensors, Sens. Actuators B 74 (2001) 100–105.
[4] C. Mouvet, R. Harris, C. Maciag, B. Luff, J. Wilkinson, J. Piehler, et al., Determination of simazine in water samples by waveguide surface plasmon resonance, Anal. Chim. Acta 338 (1997) 109–117.
[5] C.P. Cahill, K.S. Johnston, S.S. Yee, A surface plasmon resonance sensor probe based on retro-reflection, Sens. Actuators B 45 (1997) 161–166.
[6] Y.-C. Cheng, W.-K. Su, J.-H. Liou, Application of a liquid sensor based on surface plasma wave excitation to distinguish methyl alcohol from ethyl alcohol, Opt. Eng. 39 (2000) 311–314.
[7] G. Ashwell, M. Roberts, Highly selective surface plasmon resonance sensor for NO 2, Electron. Lett. 32 (1996) 2089–2091.
[8] M. Niggemann, A. Katerkamp, M. Pellmann, P. Bolsmann, J. Reinbold, K. Cammann, Remote sensing of tetrachloroethene with a micro-fibre optical gas sensor based on surface plasmon resonance spectroscopy, Sens. Actuators B 34 (1996) 328–333.
[9] C.E. Berger, J. Greve, Differential SPR immunosensing, Sens. Actuators B 63 (2000) 103–108.
[10] I. Stemmler, A. Brecht, G. Gauglitz, Compact surface plasmon resonance-transducers with spectral readout for biosensing applications, Sens. Actuators B 54 (1999) 98–105.
[11] T.T. Goodrich, H.J. Lee, R.M. Corn, Direct detection of genomic DNA by enzymatically amplified SPR imaging measurements of RNA microarrays, J. Am. Chem. Soc. 126 (2004) 4086–4087.
[12] M.A. Cooper, Optical biosensors in drug discovery, Nat. Rev. Drug Discov. 1 (2002) 515–528.
[13] Y. Fang, Label-free cell-based assays with optical biosensors in drug discovery, Assay Drug Dev. Technol. 4 (2006) 583–595.
[14] S. Fang, H.J. Lee, A.W. Wark, R.M. Corn, Attomole microarray detection of microRNAs by nanoparticle-amplified SPR imaging measurements of surface polyadenylation reactions, J. Am. Chem. Soc. 128 (2006) 14044–14046.
[15] B. Liedberg, C. Nylander, I. Lunström, Surface plasmon resonance for gas detection and biosensing, Sens. Actuators 4 (1983) 299–304.
[16] J. Homola, Surface plasmon resonance sensors for detection of chemical and biological species, Chem. Rev. 108 (2008) 462–493.
[17] R. Jorgenson, S. Yee, A fiber-optic chemical sensor based on surface plasmon resonance, Sens. Actuators B 12 (1993) 213–220.
[18] B. Gupta, R. Verma, Surface plasmon resonance-based fiber optic sensors: principle, probe designs, and some applications, J. Sens. 2009 (2009).
[19] B. Lee, S. Roh, J. Park, Current status of micro-and nano-structured optical fiber sensors, Opt. Fiber Technol. 15 (2009) 209–221.
[20] P.J. Kajenski, Tunable optical filter using long-range surface plasmons, Opt. Eng. 36 (1997) 1537–1541.
[21] Y. Wang, Voltage-induced color-selective absorption with surface plasmons, Appl. Phys. Lett. 67 (1995) 2759–2761.
[22] J.S. Schildkraut, Long-range surface plasmon electrooptic modulator, Appl. Opt. 27 (1988) 4587–4590.
[23] G.T. Sincerbox, J.C. Gordon, Small fast large-aperture light modulator using attenuated total reflection, Appl. Opt. 20 (1981) 1491–1496.
[24] Y.-T. Su, S.-J. Chen, T.-L. Yeh, A common-path phase-shift interferometry surface plasmon imaging system, Biomed. Opt. 2005 (2005) 144–151.
[25] L. Wang, R.J.H. Ng, S. Safari Dinachali, M. Jalali, Y. Yu, J.K. Yang, Large area plasmonic color palettes with expanded gamut using colloidal self-Assembly, ACS Photonics (2016).
[26] K.S. Johnston, S.R. Karlsen, C.C. Jung, S.S. Yee, New analytical technique for characterization of thin films using surface plasmon resonance, Mater. Chem. Phys. 42 (1995) 242–246.
[27] T. Akimoto, S. Sasaki, K. Ikebukuro, I. Karube, Refractive-index and thickness sensitivity in surface plasmon resonance spectroscopy, Appl. Opt. 38 (1999) 4058–4064.
[28] R. Ahmed, A.A. Rifat, A.K. Yetisen, S.H. Yun, S. Khan, H. Butt, Mode-multiplexed waveguide sensor, J. Electromagn. Waves Appl. 30 (2016) 444–455.
[29] R. Ahmed, A.A. Rifat, A.K. Yetisen, M.S. Salem, S.-H. Yun, H. Butt, Optical microring resonator based corrosion sensing, RSC Adv. 6 (2016) 56127–56133.
[30] R. Ritchie, Plasma losses by fast electrons in thin films, Phys. Rev. 106 (1957) 874.
[31] A. Otto, Excitation of nonradiative surface plasma waves in silver by the method of frustrated total reflection, Zeitschrift für Physik 216 (1968) 398–410.
[32] R. KretschmannE, Radiative decay of non-radiative surface plasmons excited by light, Z Naturforsch 23 (1968) 2135–2136.
[33] A.A. Rifat, G. Mahdiraji, Y.M. Sua, R. Ahmed, Y. Shee, F.M. Adikan, Highly sensitive multi-core flat fiber surface plasmon resonance refractive index sensor, Opt. Express 24 (2016) 2485–2495.
[34] Z. Zhu, J. Yuan, H. Zhou, J. Hu, J. Zhang, C. Wei, et al., Excitonic resonant emission-Absorption of surface plasmon in transition metal dichalcogenides for chip-level electronic-Photonic integrated circuits, ACS Photonics (2016).
[35] M. Piliarik, J. Homola, Z. Manıková, J. Čtyroký, Surface plasmon resonance sensor based on a single-mode polarization-maintaining optical fiber, Sens. Actuators B 90 (2003) 236–242.
[36] D. Monzón-Hernández, J. Villatoro, High-resolution refractive index sensing by means of a multiple-peak surface plasmon resonance optical fiber sensor, Sens. Actuators B 115 (2006) 227–231.
[37] D. Monzón-Hernández, J. Villatoro, D. Talavera, D. Luna-Moreno, Optical-fiber surface-plasmon resonance sensor with multiple resonance peaks, Appl. Opt. 43 (2004) 1216–1220.
[38] B. Gupta, A.K. Sharma, Sensitivity evaluation of a multi-layered surface plasmon resonance-based fiber optic sensor: a theoretical study, Sens. Actuators B 107 (2005) 40–46.
[39] M. Skorobogatiy, A.V. Kabashin, Photon crystal waveguide-based surface plasmon resonance biosensor, Appl. Phys. Lett. 89 (2006) 143518.
[40] A. Hassani, M. Skorobogatiy, Design of the microstructured optical fiber-based surface plasmon resonance sensors with enhanced microfluidics, Opt. Express 14 (2006) 11616–11621.
[41] B. Gauvreau, A. Hassani, M. Fassi Fehri, A. Kabashin, M.A. Skorobogatiy, Photonic bandgap fiber-based surface plasmon resonance sensors, Opt. Express 15 (2007) 11413–11426.
[42] A. Hassani, B. Gauvreau, M.F. Fehri, A. Kabashin, M. Skorobogatiy, Photonic crystal fiber and waveguide-based surface plasmon resonance sensors for application in the visible and near-IR, Electromagnetics 28 (2008) 198–213.
[43] Q. Wei, L. Shu-Guang, X. Jian-Rong, X. Xü-Jun, Z. Lei, Numerical analysis of a photonic crystal fiber based on two polarized modes for biosensing applications, Chinese Phys. B 22 (2013) 074213.
[44] B. Shuai, L. Xia, D. Liu, Coexistence of positive and negative refractive index sensitivity in the liquid-core photonic crystal fiber based plasmonic sensor, Opt. Express 20 (2012) 25858–25866.
[45] M. Tian, P. Lu, L. Chen, C. Lv, D. Liu, All-solid D-shaped photonic fiber sensor based on surface plasmon resonance, Opt. Commun. 285 (2012) 1550–1554.
[46] A. Rifat, G. Mahdiraji, D. Chow, Y. Shee, R. Ahmed, F. Adikan, Photonic crystal fiber-based surface plasmon resonance sensor with selective analyte channels and graphene-silver deposited core, Sensors 15 (2015) 11499–11510.
[47] J.N. Dash, R. Jha, SPR biosensor based on polymer PCF coated with conducting metal oxide, Ieee Photonics Technol. Lett. 26 (Mar 15) (2014) 595–598.
[48] J.N. Dash, R. Jha, Graphene-based birefringent photonic crystal fiber sensor using surface plasmon resonance, Photonics Technol. Lett. IEEE 26 (2014) 1092–1095.
[49] A.A. Rifat, G.A. Mahdiraji, Y.M. Sua, Y.G. Shee, R. Ahmed, D.M. Chow, et al., Surface plasmon resonance photonic crystal fiber biosensor: a practical sensing approach, Photonics Technol. Lett. IEEE 27 (2015) 1628–1631.

[50] L. Peng, F. Shi, G. Zhou, S. Ge, Z. Hou, C. Xia, A surface plasmon biosensor based on a D-shaped microstructured optical fiber with rectangular lattice, Photonics J. IEEE 7 (2015) 1–9.
[51] F. Shi, L. Peng, G. Zhou, X. Cang, Z. Hou, C. Xia, An elliptical core D-Shaped photonic crystal fiber-Based plasmonic sensor at upper detection limit, Plasmonics (2015) 1–6.
[52] A.K. Mishra, S.K. Mishra, B.D. Gupta, SPR based fiber optic sensor for refractive index sensing with enhanced detection accuracy and figure of merit in visible region, Opt. Commun. 344 (2015) 86–91.
[53] Q. Liu, S. Li, H. Chen, J. Li, Z. Fan, High-sensitivity plasmonic temperature sensor based on photonic crystal fiber coated with nanoscale gold film, Appl. Phy. Exp. 8 (2015) 046701.
[54] R. Otupiri, E. Akowuah, S. Haxha, Multi-channel SPR biosensor based on PCF for multi-analyte sensing applications, Opt. Express 23 (2015) 15716–15727.
[55] Y. Zhao, Z.-q. Deng, J. Li, Photonic crystal fiber based surface plasmon resonance chemical sensors, Sens. Actuators B 202 (2014) 557–567.
[56] X. Yang, Y. Lu, M. Wang, J. Yao, A photonic crystal fiber glucose sensor filled with silver nanowires, Opt. Commun. 359 (2016) 279–284.
[57] J.N. Dash, R. Jha, Highly sensitive D shaped PCF sensor based on SPR for near IR, Opt. Quantum. Electron. 48 (2016) 1–7.
[58] S.I. Azzam, M.F.O. Hameed, R.E.A. Shehata, A. Heikal, S. Obayya, Multichannel photonic crystal fiber surface plasmon resonance based sensor, Opt. Quantum. Electron. 48 (2016) 1–11.
[59] M.F.O. Hameed, M.Y. Azab, A. Heikal, S.M. El-Hefnawy, S. Obayya, Highly sensitive plasmonic photonic crystal temperature sensor filled with liquid crystal, Photonics Technol. Lett. IEEE 28 (2016) 59–62.
[60] C. Liu, F. Wang, J. Lv, T. Sun, Q. Liu, C. Fu, A highly temperature-sensitive photonic crystal fiber based on surface plasmon resonance, Opt. Commun. 359 (2016) 378–382.
[61] S. Singh, S.K. Mishra, B.D. Gupta, Sensitivity enhancement of a surface plasmon resonance based fibre optic refractive index sensor utilizing an additional layer of oxides, Sensor Actuat. A: Phys. 193 (2013) 136–140.
[62] R.K. Verma, B.D. Gupta, Surface plasmon resonance based fiber optic sensor for the IR region using a conducting metal oxide film, JOSA A 27 (2010) 846–851.
[63] R. Narayanaswamy, O.S. Wolfbeis, Optical Sensors: Industrial Environmental and Diagnostic Applications, vol. 1, Springer Science & Business Media, 2003.
[64] B. Kuswandi, R. Andres, R. Narayanaswamy, Optical fibre biosensors based on immobilised enzymes, Analyst 126 (2001) 1469–1491.
[65] M.-C. Navarrete, N. Díaz-Herrera, A. González-Cano, Ó. Esteban, Surface plasmon resonance in the visible region in sensors based on tapered optical fibers, Sens. Actuators B 190 (2014) 881–885.
[66] Y.-C. Kim, W. Peng, S. Banerji, K.S. Booksh, Tapered fiber optic surface plasmon resonance sensor for analyses of vapor and liquid phases, Opt. Lett. 30 (2005) 2218–2220.
[67] S.-F. Wang, M.-H. Chiu, R.-S. Chang, Numerical simulation of a D-type optical fiber sensor based on the Kretchmann's configuration and heterodyne interferometry, Sens. Actuators B 114 (2006) 120–126.
[68] A. Tubb, F. Payne, R. Millington, C. Lowe, Single-mode optical fibre surface plasma wave chemical sensor, Sens. Actuators B 41 (1997) 71–79.
[69] W. Peng, S. Banerji, Y.-C. Kim, K.S. Booksh, Investigation of dual-channel fiber-optic surface plasmon resonance sensing for biological applications, Opt. Lett. 30 (2005) 2988–2990.
[70] B. Špačková, J. Homola, Theoretical analysis of a fiber optic surface plasmon resonance sensor utilizing a Bragg grating, Opt. Express 17 (2009) 23254–23264.
[71] Y. Zhang, C. Zhou, L. Xia, X. Yu, D. Liu, Wagon wheel fiber based multichannel plasmonic sensor, Opt. Express 19 (2011) 22863–22873.
[72] R.A. Aoni, R. Ahmed, M.M. Alam, S.A. Razzak, Optimum design of a nearly zero ultra-flattened dispersion with lower confinement loss photonic crystal fibers for communication systems, Int. J. Sci. Eng. Res. 4 (2013).
[73] Y. Liu, Q. Liu, S. Chen, F. Cheng, H. Wang, W. Peng, Surface plasmon resonance biosensor based on smart phone platforms, Sci. Rep. 5 (2015).
[74] K. Bremer, B. Roth, Fibre optic surface plasmon resonance sensor system designed for smartphones, Opt. Express 23 (2015) 17179–17184.
[75] J. Pollet, F. Delport, K.P. Janssen, K. Jans, G. Maes, H. Pfeiffer, et al., Fiber optic SPR biosensing of DNA hybridization and DNA–protein interactions, Biosens. Bioelectron. 25 (2009) 864–869.
[76] H.-H. Jeong, N. Erdene, S.-K. Lee, D.-H. Jeong, J.-H. Park, Fabrication of fiber-optic localized surface plasmon resonance sensor and its application to detect antibody-antigen reaction of interferon-gamma, Opt. Eng. 50 (2011) 124405–124408.
[77] N.K. Sharma, M. Rani, V. Sajal, Surface plasmon resonance based fiber optic sensor with double resonance dips, Sens. Actuators B 188 (2013) 326–333.
[78] A.K. Mishra, S.K. Mishra, R.K. Verma, Graphene and beyond graphene MoS2: a new window in surface-plasmon-resonance-based fiber optic sensing, J. Phys. Chem. C 120 (2016) 2893–2900.
[79] S. Shukla, N.K. Sharma, V. Sajal, Sensitivity enhancement of a surface plasmon resonance based fiber optic sensor using ZnO thin film: a theoretical study, Sens. Actuators B 206 (2015) 463–470.
[80] X.M. Wang, C.L. Zhao, R.G. Yang, Y.R. Wang, F.F. Shi, S.Z. Jin, Tapered fiber-optic based surface plasmon resonance sensor, Appl. Mech. Mater. (2015) 23–26.
[81] M. Rani, S. Shukla, N.K. Sharma, V. Sajal, Theoretical analysis of surface plasmon resonance based fiber optic sensor using indium nitride, Optik-Int. J. Light Electron Opt. 125 (2014) 6026–6031.
[82] M. ZHANG, K. Li, P.P. Shum, X. Yu, S. Zeng, Z. Wu, et al., Graphene enhanced surface plasmon resonance fiber-optic biosensor, CLEO: Sci. Innov. (2016) SM4P.4.
[83] G. An, S. Li, X. Yan, X. Zhang, Z. Yuan, H. Wang, et al., Extra-broad photonic crystal fiber refractive index sensor based on surface plasmon resonance, Plasmonics (2016) 1–7.
[84] R.K. Gangwar, V.K. Singh, Highly sensitive surface plasmon resonance based D-shaped photonic crystal fiber refractive index sensor, Plasmonics (2016) 1–6.
[85] A.A. Rifat, R. Ahmed, A simple photonic crystal fiber based plasmonic biosensor, Int. OSA Netw. Students (IONS Dhanbad-2016) (2016) 59–60.
[86] N.M.Y. Zhang, D.J.J. Hu, P.P. Shum, Z. Wu, K. Li, T. Huang, et al., Design and analysis of surface plasmon resonance sensor based on high-birefringent microstructured optical fiber, J. Opt. 18 (2016) 065005.
[87] R. Ahmed, R.A. Aoni, D.P. Fabrizio, Design of ultra-flattened zero dispersion shifted photonic crystal fibers with lower confinement loss for telecommunication applications, CIOMP-OSA Summer Session Opt. Eng. Des. Manuf. (2013) Tu6.
[88] D.C. Allan, N.F. Borrelli, J.C. Fajardo, R.M. Fiacco, D.W. Hawtof, J.A. West, Photonic crystal fiber, ed: Google Patents (2001).
[89] T.A. Birks, J.C. Knight, P.S.J. Russell, Endlessly single-mode photonic crystal fiber, Opt. Lett. 22 (1997) 961–963.
[90] R. Ahmed, M.M. Khan, R. Ahmmed, A. Ahad, Design, simulation & optimization of 2D photonic crystal power splitter, Opt. Photonics J. 3 (2013) 13.
[91] R. Ahmmed, R. Ahmed, S.A. Razzak, Design of large negative dispersion and modal analysis for hexagonal, square, FCC and BCC photonic crystal fibers, Informatics, Electronics & Vision (ICIEV), 2013 International Conference on (2013) 1–6.
[92] R. Slavík, J. Homola, J. Čtyroký, Single-mode optical fiber surface plasmon resonance sensor, Sens. Actuators B 54 (1999) 74–79.
[93] K.M. McPeak, S.V. Jayanti, S.J. Kress, S. Meyer, S. Iotti, A. Rossinelli, et al., Plasmonic films can easily be better: rules and recipes, ACS photonics 2 (2015) 326–333.
[94] G.V. Naik, V.M. Shalaev, A. Boltasseva, Alternative plasmonic materials: beyond gold and silver, Adv. Mater. 25 (2013) 3264–3294.
[95] S.A. Zynio, A.V. Samoylov, E.R. Surovtseva, V.M. Mirsky, Y.M. Shirshov, Bimetallic layers increase sensitivity of affinity sensors based on surface plasmon resonance, Sensors 2 (2002) 62–70.
[96] N.D. Orf, O. Shapira, F. Sorin, S. Danto, M.A. Baldo, J.D. Joannopoulos, et al., Fiber draw synthesis, Proc. Natl. Acad. Sci. 108 (2011) 4743–4747.
[97] V. Kravets, R. Jalil, Y.-J. Kim, D. Ansell, D. Aznakayeva, B. Thackray, et al., Graphene-protected copper and silver plasmonics, Sci. Rep. 4 (2014).
[98] M. Schriver, W. Regan, W.J. Gannett, A.M. Zaniewski, M.F. Crommie, A. Zettl, Graphene as a long-term metal oxidation barrier: worse than nothing, ACS Nano 7 (2013) 5763–5768.
[99] D.B. Farmer, P. Avouris, Y. Li, T.F. Heinz, S.-J. Han, Ultrasensitive plasmonic detection of molecules with graphene, ACS Photonics (2016).
[100] F.J. Garcia de Abajo, Graphene plasmonics: challenges and opportunities, Acs Photonics 1 (2014) 135–152.
[101] R. Ahmed, A.A. Rifat, A.K. Yetisen, Q. Dai, S.H. Yun, H. Butt, Multiwall carbon nanotube microcavity arrays, J. Appl. Phys. 119 (2016) 113105.
[102] M.M. Huq, C.-T. Hsieh, Z.-W. Lin, C.-Y. Yuan, One-step electrophoretic fabrication of a graphene and carbon nanotube-based scaffold for manganese-based pseudocapacitors, RSC Adv. 6 (2016) 87961–87968.
[103] J.S. Bunch, S.S. Verbridge, J.S. Alden, A.M. van der Zande, J.M. Parpia, H.G. Craighead, et al., Impermeable atomic membranes from graphene sheets, Nano Lett. 8 (2008) 2458–2462.
[104] O. Salihoglu, S. Balci, C. Kocabas, Plasmon-polaritons on graphene-metal surface and their use in biosensors, Appl. Phys. Lett. 100 (2012) 213110.
[105] A.R. Davoyan, N. Engheta, Salient features of deeply subwavelength guiding of terahertz radiation in graphene-coated fibers, ACS Photonics (2016).
[106] P.R. West, S. Ishii, G.V. Naik, N.K. Emani, V.M. Shalaev, A. Boltasseva, Searching for better plasmonic materials, Laser Photonics Rev. 4 (2010) 795–808.
[107] G.H. Chan, J. Zhao, G.C. Schatz, R.P.V. Duyne, Localized surface plasmon resonance spectroscopy of triangular aluminum nanoparticles, J. Phys. Chem. C 112 (2008) 13958–13963.
[108] G.H. Chan, J. Zhao, E.M. Hicks, G.C. Schatz, R.P. Van Duyne, Plasmonic properties of copper nanoparticles fabricated by nanosphere lithography, Nano Lett. 7 (2007) 1947–1952.
[109] S.P. Polaritons, Screened plasma absorption in indium tin oxide compared to silver and gold franzen, J. Phys. Chem. C 112 (2008) 6027–6032.
[110] C. Rhodes, M. Cerruti, A. Efremenko, M. Losego, D. Aspnes, J.-P. Maria, et al., Dependence of plasmon polaritons on the thickness of indium tin oxide thin films, J. Appl. Phys. 103 (2008) 093108.
[111] D. Gao, C. Guan, Y. Wen, X. Zhong, L. Yuan, Multi-hole fiber based surface plasmon resonance sensor operated at near-infrared wavelengths, Opt. Commun. 313 (2014) 94–98.
[112] W. Qin, S. Li, Y. Yao, X. Xin, J. Xue, Analyte-filled core self-calibration microstructured optical fiber based plasmonic sensor for detecting high refractive index aqueous analyte, Opt. Laser. Eng. 58 (2014) 1–8.
[113] Z. Fan, S. Li, Q. Liu, G. An, H. Chen, J. Li, et al., High-sensitivity of refractive index sensor based on analyte-filled photonic crystal fiber with surface plasmon resonance, IEEE Photonics J. 7 (2015).

[114] X. Yu, Y. Zhang, S. Pan, P. Shum, M. Yan, Y. Leviatan, et al., A selectively coated photonic crystal fiber based surface plasmon resonance sensor, J. Opt. 12 (2010) 015005.
[115] P. Bing, J. Yao, Y. Lu, Z. Li, A surface-plasmon-resonance sensor based on photonic-crystal-fiber with large size microfluidic channels, Opt. Appl. 42 (2012) 493–501.
[116] X. Fu, Y. Lu, X. Huang, J. Yao, Surface plasmon resonance sensor based on photonic crystal fiber filled with silver nanowires, Opt. Appl. 41 (2011) 941–951.
[117] Y. Lu, M. Wang, C. Hao, Z. Zhao, J. Yao, Temperature sensing using photonic crystal fiber filled with silver nanowires and liquid, Photonics J. IEEE 6 (2014) 1–7.
[118] Y. Lu, X. Yang, M. Wang, J. Yao, Surface plasmon resonance sensor based on hollow-core PCFs filled with silver nanowires, Electron. Lett. 51 (2015) 1675–1677.
[119] F.R.M. Adikan, S.R. Sandoghchi, C.W. Yi, R.E. Simpson, M.A. Mahdi, A.S. Webb, et al., Direct UV written optical waveguides in flexible glass flat fiber chips, Selected Topics Quantum Electron. IEEE J. 18 (2012) 1534–1539.
[120] B. Shuai, L. Xia, Y. Zhang, D. Liu, A multi-core holey fiber based plasmonic sensor with large detection range and high linearity, Opt. Express 20 (2012) 5974–5986.
[121] Z. Tan, X. Li, Y. Chen, P. Fan, Improving the sensitivity of fiber surface plasmon resonance sensor by filling liquid in a hollow core photonic crystal fiber, Plasmonics 9 (2014) 167–173.
[122] J.N. Dash, R. Jha, On the performance of graphene-based D-shaped photonic crystal fibre biosensor using surface plasmon resonance, Plasmonics (2015) 1–9.
[123] D. Santos, A. Guerreiro, J. Baptista, SPR microstructured D-type optical fiber sensor configuration for refractive index measurement, SPIE (2015).
[124] N. Luan, R. Wang, W. Lv, J. Yao, Surface plasmon resonance sensor based on D-shaped microstructured optical fiber with hollow core, Opt. Express 23 (2015) 8576–8582.
[125] Z. Tan, X. Hao, Y. Shao, Y. Chen, X. Li, P. Fan, Phase modulation and structural effects in a D-shaped all-solid photonic crystal fiber surface plasmon resonance sensor, Opt. Express 22 (2014) 15049–15063.
[126] A. Hassani, M. Skorobogatiy, Photonic crystal fiber-based plasmonic sensors for the detection of biolayer thickness, JOSA B 26 (2009) 1550–1557.
[127] E.K. Akowuah, T. Gorman, H. Ademgil, S. Haxha, G.K. Robinson, J.V. Oliver, Numerical analysis of a photonic crystal fiber for biosensing applications, Quantum Electron. IEEE J. 48 (2012) 1403–1410.
[128] R. Otupiri, E. Akowuah, S. Haxha, H. Ademgil, F. AbdelMalek, A. Aggoun, A novel birefrigent photonic crystal fiber surface plasmon resonance biosensor, Photonics J. IEEE 6 (2014) 1–11.
[129] L.O. Cinteza, T.Y. Ohulchanskyy, Y. Sahoo, E.J. Bergey, R.K. Pandey, P.N. Prasad, Diacyllipid micelle-based nanocarrier for magnetically guided delivery of drugs in photodynamic therapy, Mol. Pharm. 3 (2006) 415–423.
[130] E.K. Akowuah, G. Robinson, H. Ademgil, J. Oliver, S. Haxha, T. Gorman, A Novel Compact Photonic Crystal Fibre Surface Plasmon Resonance Biosensor for an Aqueous Environment, INTECH Open Access Publisher, 2012.
[131] X. Yang, Y. Lu, M. Wang, J. Yao, An exposed-core grapefruit fibers based surface plasmon resonance sensor, Sensors 15 (2015) 17106–17114.
[132] A. Ahmmed, G. Rifat, Amouzad Mahdiraji, Rajib Ahmed, Desmond M. Chow, Y.M. Sua, Y.G. Shee, et al., Copper-graphene based photonic crystal fiber plasmonic biosensor, IEEE Photonics J. 8 (2016).
[133] A. Rifat, G.A. Mahdiraji, Y. Shee, M.J. Shawon, F.M. Adikan, A novel photonic crystal fiber biosensor using surface plasmon resonance, Procedia Eng. 140 (2016) 1–7.
[134] V. Popescu, N. Puscas, G. Perrone, Power absorption efficiency of a new microstructured plasmon optical fiber, JOSA B 29 (2012) 3039–3046.
[135] V. Popescu, N. Puscas, G. Perrone, Strong power absorption in a new microstructured holey fiber-based plasmonic sensor, JOSA B 31 (2014) 1062–1070.
[136] V. Popescu, N. Puscas, G. Perrone, Simulation of the sensing performance of a plasmonic biosensor based on birefringent solid-core microstructured optical fiber, Plasmonics (2016) 1–7.
[137] G. Amouzad Mahdiraji, D.M. Chow, S. Sandoghchi, F. Amirkhan, E. Dermosesian, K.S. Yeo, et al., Challenges and solutions in fabrication of silica-based photonic crystal fibers: an experimental study, Fiber Integr. Opt. 33 (2014) 85–104.
[138] J. Canning, E. Buckley, K. Lyttikainen, T. Ryan, Wavelength dependent leakage in a Fresnel-based air–silica structured optical fibre, Opt. Commun. 205 (2002) 95–99.
[139] T. Yajima, J. Yamamoto, F. Ishii, T. Hirooka, M. Yoshida, M. Nakazawa, Low-loss photonic crystal fiber fabricated by a slurry casting method, Opt. Express 21 (2013) 30500–30506.
[140] R.T. Bise, D.J. Trevor, Sol-gel derived microstructured fiber: fabrication and characterization, Optical Fiber Communications Conf.(OFC) (2005).
[141] K. Kiang, K. Frampton, T. Monro, R. Moore, J. Tucknott, D. Hewak, et al., Extruded single-mode non-silica glass holey optical fibres, Electron. Lett. 38 (2002) 546–547.
[142] K. Tajima, Low loss PCF by reduction of hole surface imperfection, ECOC 2007 (2007).
[143] N. Takeyasu, T. Tanaka, S. Kawata, Metal deposition deep into microstructure by electroless plating, Jpn. J. Appl. Phys. 44 (2005) L1134.
[144] P.J. Sazio, A. Amezcua-Correa, C.E. Finlayson, J.R. Hayes, T.J. Scheidemantel, N.F. Baril, et al., Microstructured optical fibers as high-pressure microfluidic reactors, Science 311 (2006) 1583–1586.
[145] J. Boehm, A. François, H. Ebendorff-Heidepriem, T.M. Monro, Chemical deposition of silver for the fabrication of surface plasmon microstructured optical fibre sensors, Plasmonics 6 (2011) 133–136.
[146] S. Sandlin, T. Kinnunen, J. Rämö, M. Sillanpää, A simple method for metal re-coating of optical fibre Bragg gratings, Surf. Coat. Technol. 201 (2006) 3061–3065.
[147] G.F. Andrade, A.G. Brolo, Nanoplasmonic structures in optical fibers, in: Nanoplasmonic Sensors, Springer, 2012, pp. 289–315.
[148] Z. Chen, Z. Dai, N. Chen, S. Liu, F. Pang, B. Lu, et al., Gold nanoparticles-Modified tapered fiber nanoprobe for remote SERS detection, Photonics Technol. Lett. IEEE 26 (2014) 777–780.
[149] M.K.K. Oo, Y. Han, R. Martini, S. Sukhishvili, H. Du, Forward-propagating surface-enhanced Raman scattering and intensity distribution in photonic crystal fiber with immobilized Ag nanoparticles, Opt. Lett. 34 (2009) 968–970.
[150] G. Shambat, S.R. Kothapalli, A. Khurana, J. Provine, T. Sarmiento, K. Cheng, et al., A photonic crystal cavity-optical fiber tip nanoparticle sensor for biomedical applications, Appl. Phys. Lett. 100 (2012) 213702.
[151] G. Taylor, A method of drawing metallic filaments and a discussion of their properties and uses, Phys. Rev. 23 (1924) 655.
[152] S. Atakaramians, S. Afshar, H. Ebendorff-Heidepriem, M. Nagel, B.M. Fischer, D. Abbott, et al., THz porous fibers: design, fabrication and experimental characterization, Opt. Express 17 (2009) 14053–14062.
[153] F. D'Angelo, Z. Mics, M. Bonn, D. Turchinovich, Ultra-broadband THz time-domain spectroscopy of common polymers using THz air photonics, Opt. Express 22 (2014) 12475–12485.

Biographies

Ahmmed A. Rifat obtained his M.Eng.Sc degree in Electrical Engineering from the University of Malaya, Malaysia in January 2016. He is currently working as a Research Assistant at Integrated Lightwave Research Group, University of Malaya, Kuala Lumpur, Malaysia. His research interest includes Surface Plasmon Resonance, Photonic Crystal Fiber, Optical Sensors and Optical Devices.

Rajib Ahmed is a PhD student at the School of Engineering, University of Birmingham, UK. His research work focusses on photonic devices based on nanostructures. His research work includes laser based nano-fabrication, Carbon Nanotubes (CNTs), Waveguide, Micro-ring Resonator, Photonic Crystals and Graphene based photonic devices modeling and implementation.

Ali K. Yetisen researches nanotechnology, photonics, biomatercials, government policy, entrepreneurship, and arts. He also lectures at Harvard-MIT Division of Health Sciences and Technology. He holds a Ph.D. degree in Chemical Engineering and Biotechnology from the University of Cambridge, where he also taught at Judge Business School. He has served as a policy advisor for the British Cabinet Office.

Haider Butt is a lecturer (assistant professor) at the School of Engineering, University of Birmingham, UK. Previously, he was a Henslow Research Fellow at the University of Cambridge, UK, from where he received his PhD in 2012. His research work focusses on photonic devices based on nanostructures like carbon nanotubes, graphene and plasmonic nanostructures. He has published over 50 peer-reviewed journal articles and has secured several prestigious research awards.

Aydin Sabouri is a postdoctoral research associate in the Micro Engineering and Nanotechnology centre at the School of Mechanical Engineering, University of Birmingham. He is experienced in various types of nanofabrication techniques and his area of expertise is focused ion beam manufacturing. His research work focuses on charge particles optics, ion-solid interactions, NEMS/MEMS devices and near-field optical devices.

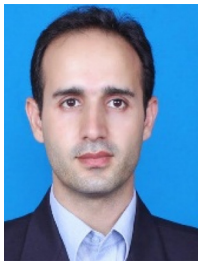

Ghafour Amouzad Mahdiraji received the Ph.D. degree in the field of communications and networks engineering major in optical communication from the Universiti Putra Malaysia (UPM), Serdang, Malaysia, in 2009. He is currently a senior researcher at Integrated Lightwave Research Group, University of Malaya, Kuala Lumpur, Malaysia. His current research interests include optical communication, radiation dosimeter and design and fabrication of microstructured optical fiber for different sensing applications.

Seok-Hyun (Andy) Yun received his Ph.D. degree in physics from Korea Advanced Institute of Science and Technology in 1997. His thesis research led to a startup company in Silicon Valley, where he managed engineering to productize fiber-optic devices for telecommunications. Currently, he is the Director of the Harvard-MIT Summer Institute for 23 Biomedical Optics. His research area includes optical imaging, photomedicine, biomaterials photonics, and biological lasers.

Faisal Rafiq Mahamd Adikan received the Ph.D. degree from the Optoelectronics Research Centre, University of Southampton, Southampton, U.K., in 2007. His Ph.D. research was focused on flat fiber and produced an international patent. He is currently the Head of the Integrated Lightwave Research Group, University of Malaya, Kuala Lumpur, Malaysia, and is involved in developing novel fabrication processes to incorporate optically active materials into a glass matrix. He specializes in glass-based integrated optical devices for use in telecommunication and sensing applications. He has published more than 100 journal and conference papers on optics and engineering education.